

FULL PAPER

Polarization modulated infrared spectroscopy: A pragmatic tool for polymer science and engineering

Stan F. S. P. Looijmans^{1,2}  | Enrico Carmeli³ | Ljiljana Puskar⁴ | Gary Ellis⁵ | Dario Cavallo³ | Patrick D. Anderson¹ | Lambert C. A. van Breemen¹ ¹Polymer Technology, Department of Mechanical Engineering, Eindhoven University of Technology, Eindhoven, The Netherlands²DPI, Eindhoven, The Netherlands³Department of Chemistry and Industrial Chemistry, University of Genova, Genova, Italy⁴Helmholtz-Zentrum für Materialien und Energie GmbH, Albert-Einstein-Straße 15, Berlin, Germany⁵Institute of Polymer Science and Technology (ICTP/CSIC), Calle de Juan de la Cierva 3, Madrid, Spain

Correspondence

Dario Cavallo, Department of Chemistry and Industrial Chemistry, University of Genova, Via Dodecaneso, 31, 16146 Genova, Italy.
Email: d.cavallo@unige.itLambert C. A. van Breemen, Polymer Technology, Department of Mechanical Engineering, Eindhoven University of Technology, P.O. Box 513, 5600 MB Eindhoven, The Netherlands.
Email: l.c.a.v.breemen@tue.nl

Funding information

Dutch Polymer Institute, Grant/Award Number: 815; Horizon 2020 Framework Programme, Grant/Award Number: 730872

Abstract

In the area of polymer crystallization, the most widely used techniques to quantify structure, morphology and molecular orientation are fundamentally based on light or X-ray scattering and absorption. In particular, synchrotron X-rays are used for detailed studies on the semicrystalline structure in polymeric materials. The technical requirements for such techniques, especially when high spatial resolution is essential, make the application of X-ray diffraction not straightforward. Direct information on the chain orientation in different semicrystalline morphologies requires rather complex sampling and analysis procedures. Surprisingly, a simple yet versatile technique based on infrared spectroscopy is hardly applied in the field of polymer crystallization. By modulating the polarization of the incident light, local anisotropy can be studied in real time on a submolecular length scale. In this article, we provide the relevant details of the polarization modulated infrared microspectroscopy technique for the study of semicrystalline materials from an engineering perspective. We demonstrate the essence of the method using as model systems spherulitic and transcrystalline morphologies and present its applicability to polymer/fiber composite technology and the study of injection-molded parts. The results provided in the present work serve to illustrate the applicability of this informative technique in the field of semicrystalline polymer science.

KEYWORDS

infrared spectroscopy, polarization modulation, structure and morphology, synchrotron radiation, vibrational linear dichroism

1 | INTRODUCTION

In numerous applications of semicrystalline materials, the desired properties of a product are only partially obtained due to the limited control over the microstructure. For polymeric materials, the local arrangement of molecules into a certain superstructure, (eg,

spherulitic, shish-kebab, transcrystalline) leads to a wide variety in both mechanical^[1,2] and physical properties.^[3] Over the last decades advanced experimental techniques for structure quantification, mostly based on scattering of electromagnetic radiation, have been developed. A combination of X-rays and visible light is often employed to access a wide range of length scales, that is, from the unit cell level

This is an open access article under the terms of the Creative Commons Attribution-NonCommercial-NoDerivs License, which permits use and distribution in any medium, provided the original work is properly cited, the use is non-commercial and no modifications or adaptations are made.

© 2020 The Authors. *Polymer Crystallization* published by Wiley Periodicals LLC.

(wide-angle X-ray diffraction, WAXD), via an intermediate, lamellar structure (small-angle X-ray scattering, SAXS) up to the spherulite size (small-angle light scattering, SALS or polarized optical microscopy, POM).^[4] The use of a high-energy photon source (ie, synchrotron X-rays) is essential to obtain information on the proper length scales, but it involves technical complications, as well as safety and cost-related issues. When anisotropic samples and morphologies are involved, the acquisition and analysis of synchrotron X-ray data require even more complex instrumentation and procedures. A much simpler and versatile complementary technique, that is, polarization modulated infrared (IR) spectroscopy, is hardly explored in the field of polymer crystallization.

Contrary to X-ray diffraction and scattering techniques, Fourier transform infrared (FTIR) spectroscopic data relates directly to the vibrational motion of a chemical bond. When these local vibrations occur in an anisotropic material, the orientation of specific bonds that absorb IR light can be quantified by measuring their polarization-dependent absorbance, that is, the vibrational linear dichroism (VLD).^[5,6] After aligning the direction of anisotropy of the material with the optical axis of the setup, the dichroic difference and dichroic ratio are obtained from the absorbance of parallel and perpendicular polarized light.

A convenient technique to study anisotropy using FTIR spectroscopy, polarization modulated infrared spectroscopy was developed almost 40 years ago,^[7] and is commonly used in the areas of surface metallurgy and coating technology.^[8,9] However, only recently it has been applied in the field of polymer science. By combining a photoelastic modulator (PEM) that alters the polarization of the IR beam at a high frequency and a conventional FTIR spectrometer, linear dichroism can be measured. With the implementation of such setup together with an IR microscope at a synchrotron facility,^[10] it is possible to measure VLD at a spatial resolution down to the diffraction limit. For semicrystalline materials, the applicability of this technique is demonstrated on a drawn polypropylene tape^[10] and a single-fiber composite.^[11]

In this article, we focus on synchrotron based microspectroscopy, as this provides a unique combination of spatial and temporal resolution.^[10,12,13] Polarization modulated synchrotron infrared microspectroscopy (PM-SIRMS) experiments are carried out at the IRIS beamline at the BESSY II synchrotron.^[14] To determine whether polarization modulated IR spectroscopy can provide similar information on chain orientation as X-ray scattering, various semicrystalline morphologies are examined; the method is illustrated on a spherulitic superstructure and two industrially relevant cases of orientation in isotactic polypropylene are discussed. The first one is the characterization of transcrystalline layers growing from a fiber surface, where we are able to quantify the difference in lamellar orientation as a result of fiber chemistry. In the second case study, an injection molded blend of polypropylene and polyethylene is studied, where we present the degree of anisotropy across the sample width for various mold temperatures and polyethylene content.

2 | MATERIALS AND METHODS

2.1 | Materials and sample preparation

To show the versatile applicability of this technique, various materials have been studied. Isotactic polypropylene (iPP) is selected to exemplify the experimental method, as it is one of the best characterized polymers in terms of crystal structure and morphology.^[15] Two homopolymer grades with weight average molar mass of 130 kg/mol (iPP-1) and 365 kg/mol (iPP-2) are kindly provided by Borealis Polyolefine GmbH (Linz, Austria). Both materials have a high isotacticity and a polydispersity index of 5.5. A thin film of approximately 40 μm in thickness is molded by manually compressing a small piece of molten polymer between two 1.1 mm thick microscope glass slides at a temperature of 220°C. The sandwiched film is cooled to room temperature and, after solidification, removed from the glass slides. Subsequently, either an uncoated 17 μm thick glass fiber, kindly provided by Nippon Electric Glass (Otsu, Japan) or a 12 μm thick aramid fiber, kindly provided by Teijin Aramids (Arnhem, The Netherlands) is introduced into this film by fixing the fiber on a microscope glass slide and melting the thin polymer film on top. To create a layer of oriented crystals on the fiber surface, that is, a cylindrical layer, the fiber is pulled through the melt at a speed of 1 mm/s for 1 second, at an isothermal crystallization temperature of 130°C, following a procedure similar to that described previously.^[16]

In addition to the above described reference samples, two recycled polypropylene/polyethylene (PP/PE) blends are provided by Borealis Polyolefine GmbH. The PP/PE composition of these materials is 90/10 and 50/50, respectively, as roughly determined by IR measurements. The large amount of impurities in these materials makes the samples nontransparent to visible light, and therefore difficult to study with conventional optical techniques such as polarized optical microscopy (POM). On the contrary, with polarization modulated spectroscopy the orientation gradient, from the skin to the core layer, can be quantitatively determined. The polymer is injection molded using a Travin TP1 mini-molder. Pellets are molten at a temperature of 200°C, well above the melting point of the highest melting phase, that is, the PP phase, to erase any thermomechanical history. Subsequently, a pneumatic piston injects the polymer melt in a dogbone-shaped mold, with a parallel section of 40 \times 5 \times 2 mm³. The force applied on the molten material by the piston can be regulated by changing the air pressure. In this study, a pressure of 7 bar was employed for every sample, which produces a theoretical apparent shear rate of about 4.1 \times 10³ s⁻¹ at the wall of the mold cavity. Different mold temperatures were used for injecting the 90/10 blend, that is, 25°C and 50°C, in order to show the ability of the technique in detecting differences in the overall orientation of the chains with different processing conditions. Subsequently, thin films (20 μm) are cut from the dogbone using a Leica RM2235 rotary microtome at room temperature. This thickness is chosen as the best compromise to obtain a clear but nonsaturated absorbance signal.

2.2 | Polarization modulation setup

The polarization modulated (PM) spectroscopy technique is based on conventional FTIR in conjunction with a photoelastic modulator which, by modulating the polarization of IR radiation at high frequency, is sensitive to anisotropy in molecular vibrations. Analogous to infrared dichroism, where a dichroic ratio is defined as the difference in the absorbance of a band when illuminated with light at two orthogonal linear polarized states (\parallel and \perp), the PM method directly generates a dichroic difference spectrum, as explained below. Although this technique can be applied using a conventional IR microscope with a global source, the data collection is often limited by long acquisition times when the focal spot dimensions drop below $100\ \mu\text{m}$, due to a strong decrease in light intensity.^[14]

However, synchrotron storage rings provide high brightness IR radiation that is not aperture limited, providing an ideal source for polarization modulated synchrotron infrared microspectroscopy.^[10] PM-SIRMS experiments are carried out at the IRIS THz/Infrared beamline, part of the Helmholtz Zentrum Berlin synchrotron facility BESSY II.^[14] The setup consists of a Nicolet Nexus 870 FTIR spectrometer coupled to a Nicolet Continuum infrared microscope and a Hinds PEM-90 II photoelastic modulator (PEM) unit to generate the orthogonally polarized light. A schematic representation of the main components together with their relative orientation is presented in Figure 1, where the arrows indicate the polarization states of the infrared light. All measurements are performed in transmission mode, where the IR beam is focused on the sample through a $32\times$ Swartzchild objective (0.65 N.A.), and the transmitted light is collected by a second $32\times$ Swartzchild condenser and guided to a liquid nitrogen cooled HgCdTe (MCT) detector. Although never applied in the field of polymer science, a similar experimental arrangement has been used to spatially and spectroscopically resolve the anisotropy on Perovskite manganites in reflectance mode.^[17,18] In this section, the photoelastic modulator (PEM) is predominantly discussed, and more

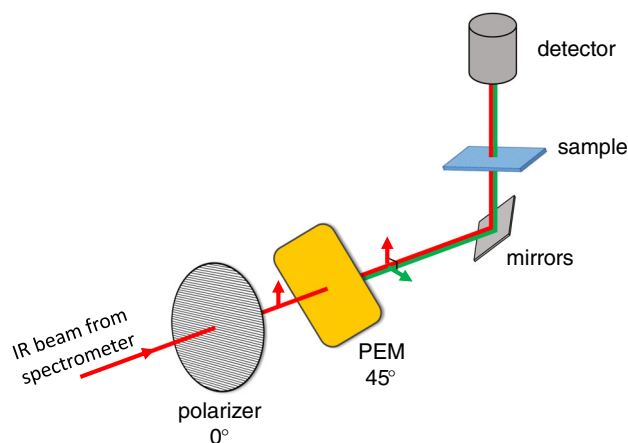


FIGURE 1 Schematic representation of the polarization modulation setup. The relative orientation of the most important optical components is indicated, together with the respective polarization of the beam

details on the beamline and standard IR equipment can be found elsewhere.^[10,12]

The PEM consists of an optical head, that is, a ZnSe crystal, which is actuated by a set of piezoelectric transducers. Stretching and compressing the crystal in an oscillating fashion creates birefringence of infrared light in the material, which induces a rotation in the plane of polarization from 45° to 0° and 90° , respectively (see Figure 1), creating two perpendicular linear polarized states. The force transducers actuating the crystal are driven by an electronic head, at a frequency of 50 kHz. The electronic head is connected to an SSD 100 synchronous scanning demodulator (GWC Technologies), which controls the optical retardation and demodulates the recorded signal from the detector. The retardation is set at $\lambda/2$, leading to a modulation between the two perpendicular linear polarization states at a frequency of 100 kHz. This retardation setting assures that a specific, pre-set wavelength is optimally retarded, that is, perfectly split into two orthogonal polarization states. The IR beam of alternating polarization is focused onto the sample and collected at the microscopes dual channel detector. The signals for the two orthogonal polarization states are split from the modulated interferogram by the demodulator into the difference ($\parallel - \perp$) and sum ($\parallel + \perp$) interferograms. As all measurements are performed in transmission mode the IR beam interacts with dipoles in the plane perpendicular to the incident light. Hence, the directions of \parallel and \perp are defined with respect to an internal reference axis of the sample rather than the surface of the sample. By switching between two orthogonal polarization states, the differential absorbance allows us to determine the local, in-plane orientation of these dipoles, and the local chain conformation from that. The difference spectrum is generally amplified to facilitate the analogue to digital conversion. The sum spectrum is used for normalization of the collected differential absorbance; since both signals are recorded simultaneously, this technique is insensitive to sample thickness variations as well as environmental changes. The Fourier transform of these two interferograms yields the normalized differential absorbance spectrum, or so-called polarization modulated dichroic difference (PMDD), defined by:

$$I_{\text{PMDD}} = \frac{I_{\text{diff}}}{I_{\text{sum}}} = \frac{I_{\parallel} - I_{\perp}}{I_{\parallel} + I_{\perp}}, \quad (1)$$

where I_{\parallel} is the intensity at the detector when the incident light is polarized parallel to the reference axis of the sample, and I_{\perp} the intensity at the detector when the light is polarized perpendicular with respect to the sample.

Spectra are acquired in the spectral range of $650 - 4000\ \text{cm}^{-1}$ and averaged over 128 scans. The use of highly brilliant synchrotron radiation allows to approach the diffraction limit of the incident light, a relatively small aperture size of $10 \times 10\ \mu\text{m}^2$ could be used, although PM-SIRMS spectra have been obtained through apertures as small as $4 \times 4\ \mu\text{m}^2$.^[11] In this case, since we are interested in the vibrational bands in the range of $800 - 1600\ \text{cm}^{-1}$, the peak retardation frequency is set at a wavenumber of $1200\ \text{cm}^{-1}$. It should be noted that bilinear dichroism is solely achieved at this specific frequency, and

that spectral bands far from the set-point lack complete optical correction. The recorded PMDD signal can however, be transformed into a true dichroic difference.^[19] The orientation direction in all the samples, that is, transcrystalline growth and injection direction respectively, is aligned with the vertical axis of the microscope stage, that coincides with one of the polarization directions of the oscillating IR light.

3 | RESULTS AND DISCUSSION

3.1 | Method illustration

In conventional measurements of linear dichroism, a polarizer is used to rotate the plane of polarization incident on the sample. However, since synchrotron IR radiation from a bending magnet source is highly polarized, rotation of the sample is necessary in order to obtain dichroic information. Thus, conventional dichroism measurements have several disadvantages; as the sample needs to be rotated with respect to the polarization of the incident light, lateral inaccuracies may arise from difficult sample positioning. A changing environment over time, such as is the case for synchrotron sources without top-up mode where the current diminishes over time, may lead to an increase in the noise in the detector signal. In addition, each sample point needs to be measured in duplicate. Using PM-SIRMS most of these challenges disappear. With this technique solely a single measurement per sample point suffices; as the oscillation frequency of the PEM is much higher than the mirror velocity of the spectrometer, the absorbance of both parallel (||) and perpendicular (⊥) polarized light is recorded simultaneously. Therewith, the acquisition time is strongly reduced, no artificial sample or polarizer rotation is needed and environmental changes are intrinsically canceled out. Hence, large 2D area maps can be collected at high spatial resolution using a motorized x,y-stage without the need for background determination.

At each measurement position the demodulated signals coming from the dual channel detector correspond to the raw difference

spectrum (I_{diff}) and the raw sum spectrum (I_{sum}). An example is given in Figure 2 of spectra obtained from an α -phase iPP spherulitic superstructure (iPP-1), where raw I_{diff} and I_{sum} spectra are presented in Figure 2A and the (amplification corrected) ratio of these two spectra, that is, the PMDD spectrum, is compared in Figure 2B between locations in the spherulite where the lamellae are oriented vertically and horizontally with respect to the microscope stage reference axis. A standard FTIR spectrum is included as a reference. Even though the spherulitic morphology can be considered macroscopically isotropic, the majority of the molecular vibrations exhibit VLD that can be observed at a length scale of 10 μm ; this local anisotropy is related to the radial growth of fibrils of lamellae, with the polymer chain axis perpendicular to the lamellar fold surface. Solely in a perfectly isotropic sample, that is, isotropic at all length scales, the differential absorbance signal is by definition equal to zero.

Furthermore, the differential absorbance may cancel out when the sample is misaligned to the polarization of the incident light; if a highly anisotropic material is subjected to radiation of two perpendicular linearly polarized states, spectral symmetry is introduced when this sample is placed at an angle of 45° with respect to either of the polarization directions.^[10] In this case, the bilinear states cancel each other and the corresponding PMDD spectrum will be zero. Note that this phenomenon is an artifact of the combination of the setup and sample orientation, and not an inherent feature of the microstructure. It may be compared to the well-known Maltese cross that is observed when a spherulite is placed between cross-polarizers,^[20] where rotating the polarization direction leads to a change in the location of the bright and dark areas.

To highlight the importance of sample alignment, an azimuthal scan was made on the circumference of a spherulite, at two different radii. In Figure 3A these locations are indicated by points, but it should be noted that in practice the IR beam presents a square shape on the sample with an aperture size of 10 \times 10 μm^2 , leading to some overlap of the true measured areas. The azimuthal angle is defined with respect to the horizontal axis of the microscope stage. The PMDD intensity of the rocking motion of the methyl-side group at 900 cm^{-1} is shown in Figure 3B. For both values of the scan radius the PMDD

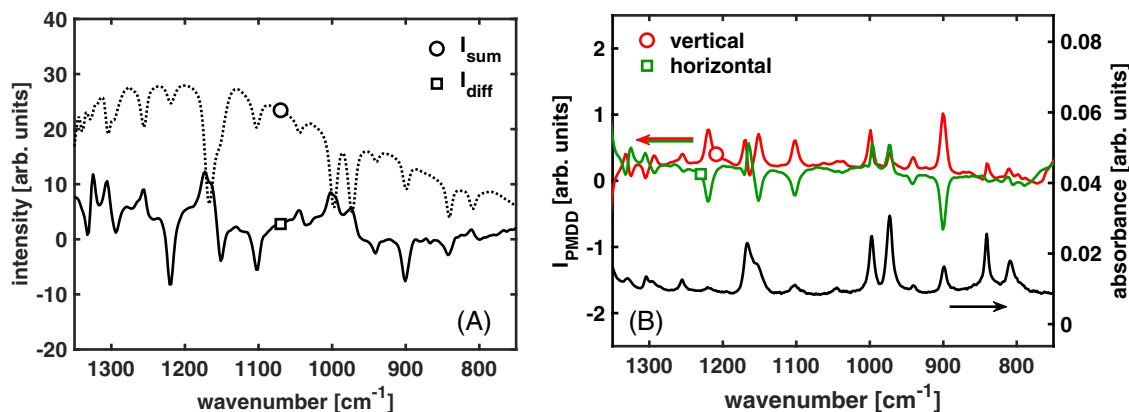


FIGURE 2 A, Typical raw difference (I_{diff}) and sum (I_{sum}) spectra recorded from an α -phase iPP spherulite. B, PMDD spectra (defined by Equation (1)) recorded from vertical and horizontal oriented lamellae of an α -phase iPP spherulite. A conventional FTIR absorbance spectrum is provided as reference

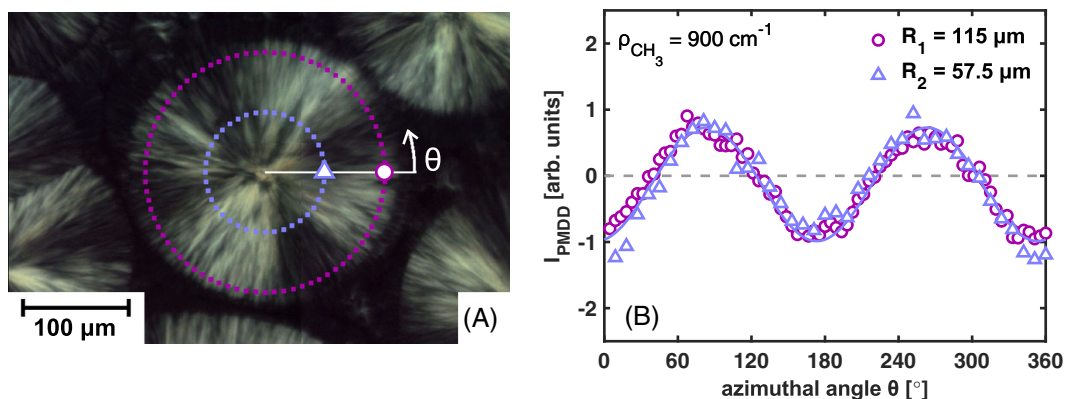


FIGURE 3 A, Locations on the periphery of an iPP-1 spherulite, crystallized isothermally at a temperature of 130°C, where PMDD spectra are recorded. B, Peak intensity of the 900 cm^{-1} spectral band, that is, the rocking motion of the methyl-group, at the corresponding locations depicted in A

intensity follows a sinusoidal trend around zero intensity, with a period of 180°. The internal rotation symmetry within a spherulite implies that the observed sinusoidal trend is a characteristic of the optical setup. Hence, to precisely capture the differential absorbance, the reference axis within the sample (eg, stretching direction, flow direction, etc.) has to be aligned with either the maximum or minimum of this sine wave. However, as can be deduced from Figure 3B, the optical axis of the setup coincide fairly well with the horizontal and vertical axis of the microscope stage. Due to the lack of a controlled rotary stage, possible misalignment is in this case prevented by aligning our samples with respect to the microscope stage, therewith accepting the small error in optical precision.

For a large enough radius, compared to the spot size of the IR beam, PM-SIRMS is sensitive to the lamellar orientation, even within a macroscopically isotropic sample. When the radius of a spherulite becomes too small, the depicted sinusoidal curve flattens, and anisotropy can no longer be detected. To show this feature, a second sample (iPP-2) is selected for validation, of which the morphology is shown in Figure 4. The structure consists of an aramid fiber with a transcrystalline-like, that is cylindritic, layer grown under the influence of relative shear. The distinction between a transcrystalline and cylindritic morphology is caused by the difference in nucleation mechanism as defined by Varga and Karger-Kocsis.^[21] In literature however, the term transcrystalline is often used for both superstructures. As the PM-SIRMS techniques apply for both morphologies, we name the structure transcrystalline-like (TCL) in the remainder of this work. In this case, the TCL is surrounded by spherulites that crystallized under quiescent conditions at a larger distance from the fiber surface.

Radial scans are acquired over the vertical and horizontal axis of such a spherulite respectively. The differential absorbance related to the rocking motion of the CH_3 side-group is presented in Figure 5A. Up to approximately 30 – 40 μm distance from the spherulite center the PMDD intensity is constant, so the local degree of orientation can be accurately determined with an aperture size of 10 μm . Closer to the center, the length-scale of unidirectional orientation is too small, and the signal becomes increasingly more isotropic. In the center of

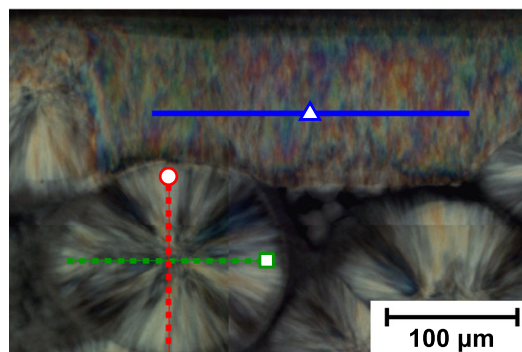


FIGURE 4 Transcrystalline-like morphology of iPP-2 isothermally crystallized around an aramid fiber, surrounded by isotropic spherulites. The markers indicate the location of the PMDD spectra presented in Figures 2B and 5B, respectively

the spherulite, the rotational symmetry of the local structure makes the recorded differential absorbance signal disappear.

So far predominantly the quasi-isotropic spherulitic morphology is discussed. As shown in Figure 4, the crystalline superstructure of iPP can also be unidirectional. In this case, the TCL is composed of the highly birefringent β -phase crystals grown in the direction perpendicular to the fiber surface.^[22] An example of a PMDD spectrum measured in this oriented β -phase is presented in Figure 5B. Compared to the previously discussed α -phase spectra (Figure 2B), it is clear that the differential absorbance signal is much stronger. First, the TCL comprises a structure that is generated by “actively” orienting the polypropylene molecules close to the fiber by applying a shear flow. In this way, a growth front parallel to the fiber surface is created, and the growth proceeds perpendicular to the fiber axis. Since a TCL morphology lacks the curvature that is intrinsically related to the spherulitic structure, the orientation of individual lamellae is more spatially correlated, leading to a substantially more anisotropic absorbance. More importantly, the inherent difference between α - and β -phases of iPP needs to be considered; whereas in α -iPP cross-hatching due to the

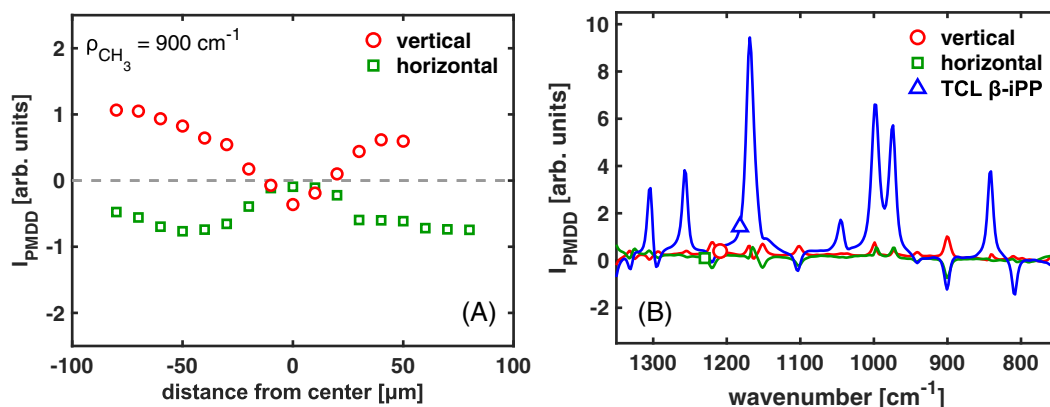


FIGURE 5 A, Line scans along the vertical and horizontal direction of an iPP-2 α -phase spherulite as indicated in Figure 4. B, Comparison of a PMDD spectrum taken in the highly birefringent β -phase TCL structure with the spectra taken in the spherulite (see Figure 4 for the measurement positions). Note the different scale of the y-axis as compared to Figure 2B

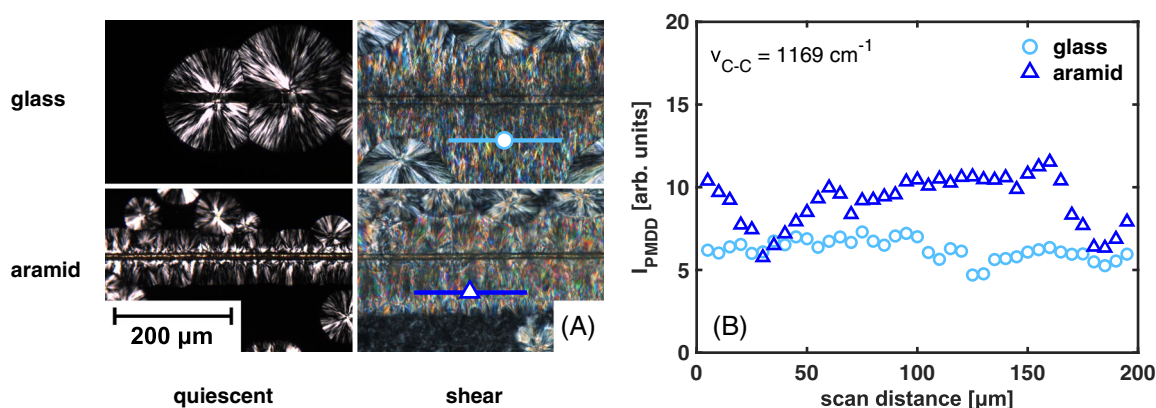


FIGURE 6 A, Morphology of iPP-1 around a glass and aramid fiber after isothermal crystallization at 130°C under the indicated conditions (quiescent or shear-induced crystallization). The location of the PMDD line scans in the case of shear flow is indicated. B, Differential absorbance of the carbon-carbon vibration, that is, backbone stretch, as a function of scan distance along the lines shown in A

formation of daughter lamellae almost perpendicular to the parent lamellae is an important morphological feature,^[23] it is not present in β -iPP. The lack of cross-hatching in the latter crystal phase, which implies the formation of secondary lamellae at similar angles to the parent lamellae, contributes to a large extent in the correlation of lamellar orientation in β -phase iPP, and hence to the significant differential absorbance observed. This inherent difference between various crystal modifications is a crucial consideration when comparing differential absorbance data, as it is not counterbalanced by the normalization procedure of PM-SIRMS.

3.2 | Structure quantification of oriented morphologies

After demonstrating the applicability of polarization modulated infrared spectroscopy to quantify orientation in polymer crystallization, two practical examples are now discussed; the technique is applied first to single-fiber composites and thereafter to injection molded parts.

Under the influence of a shear flow, a cylindrical layer is created around an uncoated glass fiber and an aramid fiber.^[24] As shown in Figure 6A, under quiescent crystallization conditions it is relatively straightforward to compare the morphology around the two different fibers by direct counting of the nuclei in time. Contrary, in the case of shear flow the extreme nucleation density at the fiber surface makes it practically impossible to quantitatively distinguish between the β -phase TCL layers. Although this particular morphology is extensively studied,^[25–29] the quantification of orientation around such interfaces is certainly not straightforward. Recently, Zhao et al.^[30] showed that the effect of crystallization temperature on the orientation within a TCL can be quantified using the dichroic ratio R . This parameter is defined as the ratio of the parallel (A_{\parallel}) over the perpendicular absorbance (A_{\perp}), i.e.

$$R = \frac{A_{\parallel}}{A_{\perp}}. \quad (2)$$

We performed a similar experiment using PM-SIRMS to quantify the differential absorbance of the TCL around the different fibers. Scans with a length of 200 μm and step size of 5 μm are made at a

distance of 50 μm parallel to the fiber surface, as indicated by the right-hand panels of Figure 6A. To measure the degree of lamellar orientation, the peak intensity of the carbon-carbon stretch vibrational band at 1169 cm^{-1} is examined. For both the neat glass and aramid fiber, these results are presented in Figure 6B. Over the entire length of the scan, the anisotropy in the TCL around the aramid fiber is significantly stronger than in the TCL around the glass fiber. In some regions a decrease in the anisotropy can be seen, which is attributed to the peculiar morphology of β -phase spherulites, exhibiting banding along the radius.^[31] Here, the twisting of β -phase lamellae causes a periodic variation of chain orientation with distance from the fiber surface.^[11] The regions where the PMDD intensity is low correspond to the area in the sample where the lamellae are predominantly “flat-on,” hence with the polymer chains on the same axis as the IR beam. Given that the correlation between the lamellae originating from different nuclei along the fiber surface is not perfect, by performing a line scan at a constant distance from the fiber, “flat-on” lamellae might occasionally be found next to the “edge-on” (with their chain axis lying in the plane of the sample and corresponding to the maximum PMDD intensity). However, because the difference in dichroic absorbance between the two fibers is large compared to the fluctuations within a sample, an average value for each sample can be used to quantify the degree of orientation. Note that polarization modulated infrared spectroscopy is by definition normalized to the incident light intensity and sample thickness, and hence allows for straightforward inter-sample comparison.

PM-SIRMS has both the spatial precision (no lateral misalignment) and spatial contrast (aperture of $10\ \mu\text{m}$) to be suitable for accurate determination of the local anisotropy in these systems. The mean PMDD intensity of the vibrational band corresponding to the polymer backbone stretch is directly related to the nucleation density; with increasing number of nuclei, transverse growth of the crystallites is increasingly constrained by neighboring crystallites. Hence, the growth is on average more aligned perpendicular to the fiber surface, leading to higher average chain orientation. The stronger differential absorbance of the TCL around the aramid fiber as compared to the glass fiber correlates well with the difference in nucleation density observed in these systems under quiescent crystallization conditions. Hence, contrary to the general perception in composites technology, the influence of fiber/matrix interaction is still present in the case of relative shear flow.

In a second example, the orientation within the cross-section of an injection molded product is determined. Tensile bars are injection molded using a pneumatic molding device. A molten PP/PE blend is pushed from top to bottom in a dog-bone shaped cavity. In the parallel section of the mold, the complex flow profile leads to an inhomogeneous morphology.^[4,32–35] Depending on the mold temperature, a thin layer of material is quenched at the mold surface. Due to the non-Newtonian flow behavior of a polymer melt, going towards the core, a strong shear layer is encountered first, before the isotropic core is reached. This particular skin-core morphology has been extensively studied for neat iPP systems using polarized optical microscopy (POM) and X-ray scattering.^[4] In a recycled polymer blend, as well as

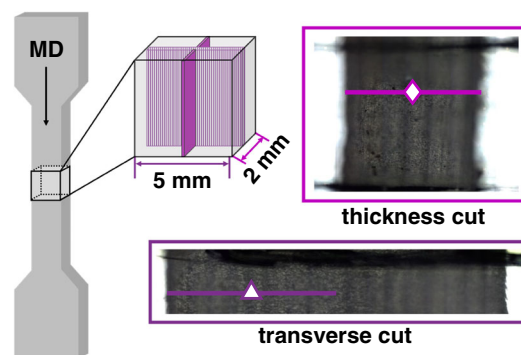


FIGURE 7 Schematic representation of the dog-bone shaped tensile bar. The machine direction (MD) is indicated by the arrow. Thin sections are microtomed from the core of the sample along the thickness and transverse direction. In an example of such section, the respective line scans made with PM-SIRMS are indicated. For the cuts along thickness direction, the total sample width is span, whereas for the cut in transverse direction half of the sample width is mapped

in colored polymer batches, the use of POM is limited by the lower transparency of the sample towards light in the visible part of the electromagnetic spectrum. With PM-SIRMS this problem can be circumvented, and direct assessment of local orientation is possible.

Thin plaques are taken from the core of the tensile bars (PP/PE blend ratios of 90/10 and 50/50). As illustrated in Figure 7, a layer with a thickness of $20\ \mu\text{m}$ is cut along the transverse and thickness direction from the center part of the specimen. Given the dimensions of the layers, scans of $2.5\ \text{mm}$ (half sample width) are made on the transverse section, while the complete sample width is scanned for the cut along the thickness direction of the bar. Individual micrographs are acquired with a $32\times$ microscope objective and stitched together to form the sample images as shown in Figure 7. Therefore, the limited transparency of the plaques is not due to an improper choice of microscope magnification, but rather the result of the blend morphology and mixture coloring.

Infrared line scans are employed at four different locations on the transverse cut 90/10 sample. For two mold temperatures, 25°C and 50°C , the PMDD spectra are acquired from skin to core. The differential absorbance of the 1169 cm^{-1} spectral band, generated by the oriented crystalline PP chains, is shown in Figure 8A as function of the scan distance, that is, the distance from the skin towards the core of the sample. For both mold temperatures, a clear increase of the PMDD intensity close to the skin is observed. This increase in differential absorbance indicates a layer where the structure is highly oriented in the injection direction. The thickness of the oriented shear layer, approximately $200\ \mu\text{m}$, is comparable to the typical values reported for neat PP and PE on the basis of microfocus X-ray diffraction.^[4] Furthermore, a clear difference between the imposed mold temperatures can be observed; with increasing mold temperature, the polymer melt is cooled less rapidly and hence the chains have more time for relaxing the stress introduced during the mold filling stage. This manifests itself by an overall decrease in PMDD intensity for the sample molded at 50°C as compared to that at 25°C . Note that

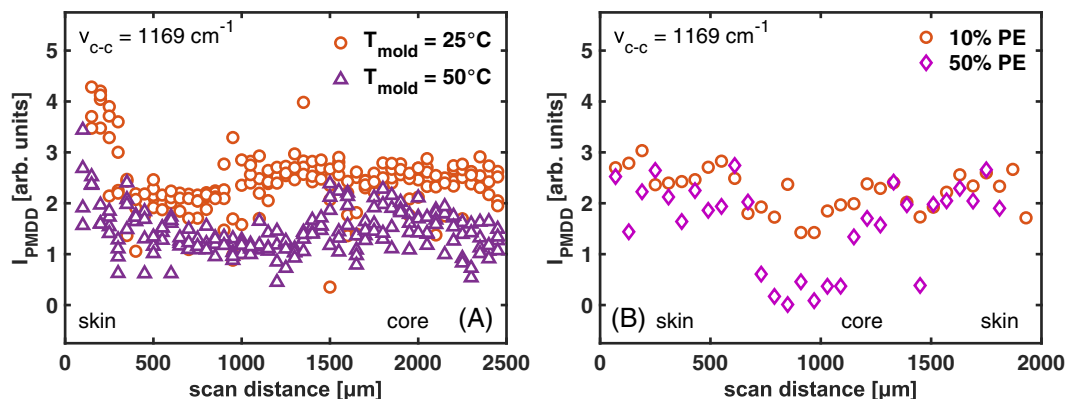


FIGURE 8 Line scans of the PMDD intensity (1169 cm^{-1} band) measured, A, along the transverse direction of the 90/10 PP/PE blend for two different mold temperatures, and B, along the thickness direction of various PP/PE blends. In the latter case, the mold temperature is 25°C

although the orientation varies over the width of the sample, the sample is anisotropic over the whole area, as the PMDD measured is always above zero.

Besides changing the mold temperature, the degree of orientation over the thickness is examined for PP/PE blends of different composition. In Figure 8B the PMDD intensity of the 1169 cm^{-1} spectral band is presented across the thickness direction of the tensile bars. The 90/10 sample does not show a clear shear layer, but rather a constant degree of orientation along the thickness. With increasing amount of polyethylene in the sample (50/50 ratio) the core layer becomes practically isotropic, while the amount of orientation at the walls is not affected. This indicates that a larger fraction of polyethylene accelerates the relaxation of the melt rather than causing wall slip in the mold.

These results show that PM-SIRMS is a versatile technique that is well capable of detecting variations in structural alignment within a sample at adequate spatial resolution, and can be utilized to detect orientation differences between various samples. Due to its normalization procedure, most inter-sample discrepancies and environmental changes are canceled out, leaving only the real structural features.

4 | CONCLUSIONS

In this work, we used a technique that is relatively unexplored in the field of polymer science, and applied it to several orientation related challenges. By changing the polarization of the infrared light, and subsequently demodulating the detector signal, a measure of the differential absorbance is obtained. Combining the polarization modulation setup with synchrotron infrared microspectroscopy, crystal orientation at a length scale down to the diffraction limit can be measured. For infrared radiation, this corresponds to micrometer-sized domains, for example, blend morphologies, semicrystalline superstructures or composite materials. The nature of vibrational spectroscopy, however, is that it provides valuable information at a molecular level, albeit averaged over a relatively large material volume.

The spherulitic morphology of an isotropic polypropylene sample is studied. The rotational symmetry of this structure is used to validate

and calibrate the PM-SIRMS setup, and a comparison between the α - and β -phase of polypropylene was made. Subsequently, two industrially relevant cases are discussed.

The morphology of an iPP melt around various fibers crystallizing under shear flow conditions is examined with polarization modulated infrared microspectroscopy. It is shown that the influence of fiber/matrix compatibility is still present in the case of shear flow, and that the lamellar orientation in the transcrystalline layer correlates well with the morphological differences observed in quiescent conditions.

The orientation of nontransparent, injection molded PP/PE blends is measured from skin to core. The presented technique is able to capture the highly oriented shear layer of such systems, as well as the decrease in overall orientation resulting from an increased mold temperature or polyethylene fraction.

In summary, we demonstrate the versatility and suitability of this technique for a variety of problems in polymer crystallization, with the aim to disseminate this useful tool among the polymer community.

ACKNOWLEDGMENTS

This research forms part of the research programme of DPI, project #815 PROFIT. We thank HZB for the allocation of synchrotron radiation beamtime, and in particular the staff of the IRIS beamline. The research leading to this result has been supported by the project CALIPSOpus under the Grant Agreement 730872 from the EU Framework Programme for Research and Innovation HORIZON 2020.

ORCID

Stan F. S. P. Looijmans  <https://orcid.org/0000-0002-4148-8351>
Lambert C. A. van Breemen  <https://orcid.org/0000-0002-0610-1908>

REFERENCES

- [1] T. B. van Erp, C. T. Reynolds, T. Peijs, J. A. W. van Dommelen, L. E. Govaert, *J. Polym. Sci. B* **2009**, *47*, 2026. <https://doi.org/10.1002/polb.21801>.
- [2] D. J. A. Senden, G. W. M. Peters, L. E. Govaert, J. A. W. van Dommelen, *Polymer* **2013**, *54*, 5899. <https://doi.org/10.1016/j.polymer.2013.08.047>.

- [3] A. Rodger, R. Marrington, M. A. Geeves, M. Hicks, L. de Alwis, D. J. Halsall, T. R. Dafforn, *Phys. Chem. Chem. Phys.* **2006**, *8*, 3161. <https://doi.org/10.1039/B604810M>.
- [4] B. A. G. Schrauwen, L. C. A. van Breemen, A. B. Spoelstra, L. E. Govaert, G. W. M. Peters, H. E. H. Meijer, *Macromolecules* **2004**, *37*, 8618. <https://doi.org/10.1021/ma048884k>.
- [5] I. Noda, A. E. Dowrey, C. Marcott, *Appl. Spectrosc.* **1988**, *42*, 203. <https://doi.org/10.1366/0003702884428310>.
- [6] H. W. Siesler, *Adv. Polym. Sci.* **1984**, *65*, 1. <https://doi.org/10.1007/BFb0017101>.
- [7] C. Marcott, *Appl. Spectrosc.* **1984**, *38*, 442. <https://doi.org/10.1366/0003702844555322>.
- [8] B. J. Barner, M. J. Green, E. I. Saez, R. M. Corn, *Anal. Chem.* **1991**, *63*, 55. <https://doi.org/10.1021/ac00001a010>.
- [9] L. Harms, I. Brand, *Vibr. Spectrosc.* **2018**, *97*, 106. <https://doi.org/10.1016/j.vibspec.2018.06.006>.
- [10] M. Schmidt, U. Schade, M. Grunze, *Infrared Phys. Technol.* **2006**, *49*, 69. <https://doi.org/10.1016/j.infrared.2006.01.005>.
- [11] G. Santoro, M. Schmidt, U. Schade, C. Marco, G. Ellis, *J. Phys.: Conf. Ser.* **2012**, *359*, 012005. <https://doi.org/10.1088/1742-6596/359/1/012005>.
- [12] U. Schade, A. Röseler, E. H. Korte, F. Bartl, T. Hofmann, K. P. Noll, W. B. Peatman, *Rev. Sci. Instrum.* **2002**, *73*, 1568. <https://doi.org/10.1063/1.1423781>.
- [13] G. J. Ellis, M. C. Martin, *Eur. Polym. J.* **2016**, *81*, 505. <https://doi.org/10.1016/j.eurpolymj.2016.02.013>.
- [14] L. Puskar, U. Schade, *J. Large-Scale Res. Facil.* **2016**, *2*, A95. <https://doi.org/10.17815/jlsrf-2-95>.
- [15] G. Grosso, E. M. Troisi, N. O. Jaensson, G. W. M. Peters, P. D. Anderson, *Polymer* **2019**, *182*, 121806. <https://doi.org/10.1016/j.polymer.2019.121806>.
- [16] G. Ellis, M. A. Gómez, C. Marco, *J. Macromol. Sci. B: Phys.* **2004**, *43*, 191. <https://doi.org/10.1081/MB-120027758>.
- [17] M. Schmidt, J. S. Lee, M. Grunze, K. H. Kim, U. Schade, *Appl. Spectrosc.* **2008**, *62*, 171. <https://doi.org/10.1366/000370208783575500>.
- [18] J. S. Lee, M. Schmidt, U. Schade, C. S. W, K. H. Kim, *Phys. Rev. B* **2009**, *79*, 073102. <https://doi.org/10.1103/PhysRevB.79.073102>.
- [19] T. Buffeteau, B. Desbat, M. Pézolet, J. M. Turllet, *J. Chim. Phys. Physicochim. Biol.* **1993**, *90*, 1467. <https://doi.org/10.1051/jcp/1993901467>.
- [20] B. Crist, J. M. Schultz, *Prog. Polym. Sci.* **2016**, *56*, 1. <https://doi.org/10.1016/j.progpolymsci.2015.11.006>.
- [21] J. Varga, J. Karger-Kocsis, *Polymer* **1995**, *36*, 4877. [https://doi.org/10.1016/0032-3861\(95\)99305-E](https://doi.org/10.1016/0032-3861(95)99305-E).
- [22] J. Torre, M. Cortázar, M. A. Gómez, C. Marco, G. Ellis, C. Riekkel, P. Dumas, *Macromolecules* **2006**, *39*, 5564. <https://doi.org/10.1021/ma060760f>.
- [23] K. Yamada, S. Matsumoto, K. Tagashira, M. Hikosaka, *Polymer* **1998**, *39*, 5327. [https://doi.org/10.1016/S0032-3861\(97\)10208-7](https://doi.org/10.1016/S0032-3861(97)10208-7).
- [24] J. Varga, J. Karger-Kocsis, *J. Polym. Sci. B* **1996**, *34*, 657. [https://doi.org/10.1002/\(SICI\)1099-0488\(199603\)34:4<657::AID-POLB6>3.0.CO;2-N](https://doi.org/10.1002/(SICI)1099-0488(199603)34:4<657::AID-POLB6>3.0.CO;2-N).
- [25] A. M. Chatterjee, F. P. Price, *J. Polym. Sci.: Polym. Phys. Ed.* **1975**, *13*, 2369. <https://doi.org/10.1002/pol.1975.180131211>.
- [26] H. Ishida, P. Bussi, *Macromolecules* **1991**, *24*, 3569. <https://doi.org/10.1021/ma00012a017>.
- [27] C. Wang, C.-R. Liu, *Polymer* **1999**, *40*, 289. [https://doi.org/10.1016/S0032-3861\(98\)00240-7](https://doi.org/10.1016/S0032-3861(98)00240-7).
- [28] H. Quan, Z.-M. Li, M.-B. Yang, R. Huang, *Compos. Sci. Technol.* **2005**, *65*, 999. <https://doi.org/10.1016/j.compscitech.2004.11.015>.
- [29] C. Wang, L. F-H, W.-H. Huang, *Polymer* **2011**, *52*, 1326. <https://doi.org/10.1016/j.polymer.2011.01.036>.
- [30] J. Zhao, J. Zhang, M. Jing, G. Sui, D. Liu, K. Wang, Q. Fu, *J. Polym. Sci. B* **2019**, *57*, 368. <https://doi.org/10.1002/polb.24790>.
- [31] J. Varga, *J. Macromol. Sci. B: Phys.* **2002**, *41*, 1121. <https://doi.org/10.1081/MB-120013089>.
- [32] S. S. Katti, J. M. Schultz, *Polym. Eng. Sci.* **1982**, *22*, 1001. <https://doi.org/10.1002/pen.760221602>.
- [33] R. Pantani, I. Coccorullo, V. Speranza, G. Titomanlio, *Prog. Polym. Sci.* **2005**, *30*, 1185. <https://doi.org/10.1016/j.progpolymsci.2005.09.001>.
- [34] J.-W. Housmans, M. Gahleitner, G. W. M. Peters, H. E. H. Meijer, *Polymer* **2009**, *50*, 2304. <https://doi.org/10.1016/j.polymer.2009.02.050>.
- [35] R. Pantani, V. Speranza, G. Titomanlio, *Eur. Polym. J.* **2017**, *97*, 220. <https://doi.org/10.1016/j.eurpolymj.2017.10.012>.

How to cite this article: Looijmans SFSP, Carmeli E, Puskar L, et al. Polarization modulated infrared spectroscopy: A pragmatic tool for polymer science and engineering. *Polymer Crystallization*. 2020;3:e10138. <https://doi.org/10.1002/pcr2.10138>